JOURNAL OF VIROLOGY, June 1976, p. 1016-1023

Vol. 18, No. 3
Printed in U.S.A.

Excision and Duplication of su3$^+$-Transducing Fragments Carried by Bacteriophage ϕ80

I. Novel Structure of ϕ80*sus*2psu3$^+$ DNA Molecule

HIDEO YAMAGISHI,* HACHIRO INOKUCHI, AND HARUO OZEKI

Department of Biophysics, Faculty of Science, Kyoto University, Kyoto, Japan

Received for publication 10 December 1975

DNA molecules of ϕ80*sus*2psu3$^+$ and ϕ80dsu3$^+$ isolated by Andoh and Ozeki (1968) were studied by the electron microscope heteroduplex method. The ϕ80*sus*2psu3$^+$ and ϕ80dsu3$^+$ DNA lengths were found to be 108.7 and 103.3% of the ϕ80 DNA, respectively. The ϕ80*sus*2psu3$^+$/ϕ80 heteroduplex shows an insertion loop of 8.7% of the ϕ80 DNA which migrates from 7.7 to 9.7%, as measured relative to the left (0%) and right (100%) termini of the mature ϕ80 DNA molecule. The region of loop migration occupies the central region of the ϕ80 head gene cluster. The presence of su3$^+$-containing *Escherichia coli* DNA of 6.7% ϕ80 unit flanked by two homologous regions of phage DNA of 2.0% of ϕ80 unit gives rise to a movable insertion loop. In ϕ80dsu3$^+$, from which ϕ80-*sus*2psu3$^+$ was derived, 50.5% of the ϕ80 DNA at the left arm was replaced by *E. coli* DNA containing the su3$^+$ gene, equivalent to about 53.8% ϕ80 unit in length. The ϕ80*sus*2psu3$^+$/ϕ80dsu3$^+$ heteroduplex appears as a double-stranded molecule that bifurcates into two clearly visible single-stranded regions, rejoins, bifurcates, and rejoins again. The middle double-stranded stretches of 6.7% ϕ80 unit correspond to the *E. coli* DNA inserted in ϕ80*sus*2psu3$^+$. Therefore the transducing fragment carried by ϕ80*sus*2psu3$^+$ originates from the inside region of the transducing fragment of defective phage ϕ80dsu3$^+$ by at least two illegitimate recombination events.

A plaque-forming transducing phage of ϕ80, carrying the su3$^+$ suppressor gene of *Escherichia coli*, has been isolated independently by Andoh and Ozeki (1) and Russell et al. (15). The former strain carries the *sus*2 amber mutation in one of the genes for the phage tail, which is suppressed by su3$^+$ contained in the transducing fragment. Therefore, it is phenotypically *sus*2$^+$ and is described as ϕ80*sus*2psu3$^+$. Strain ϕ80*sus*2psu3$^+$ has an interesting but puzzling characteristic: vegetative growth of ϕ80-*sus*2psu3$^+$ produces ϕ80*sus*2 progeny phages that have lost suppressor activity at high frequency, even after several cycles of single-plaque isolation. The loss of the suppressor activity has been attributed to the loss of an entire transducing fragment and has been explained by assuming the presence of a duplicated region of the phage genome at either end of the transducing fragment (1). To examine this model, the location, size, and structure of the transducing fragment are studied by electron micrographic mapping of heteroduplex DNA.

(A preliminary account of this work has already been presented [H. Yamagishi, H. Ozeki, and M. Ikenaga, Jpn. J. Genet. 48:454, 1973].)

MATERIALS AND METHODS

Bacteriophage strains. Bacteriophages ϕ80*sus*2, ϕ80*sus*2psu3$^+$, and ϕ80dsu3$^+$ are those described by Andoh and Ozeki (1). Mutant phage ϕ80*sus*2 contains an amber mutation in gene *8*, one of the genes for the phage tail (17). Phage ϕ80*sus*2*imm*$^\lambda$psu3$^+$ was constructed in this laboratory by crossing ϕ80*sus*2psu3$^+$ and wild-type λ. Its chromosome is composed mainly of ϕ80*sus*2psu3$^+$, and only the region comprising genes *red-15-imm*^{80}*-14-16* is replaced by λ DNA. In the present study, the buoyant density in CsCl was determined to be 1.493 g/cm^3 for ϕ80*sus*2, 1.504 g/cm^3 for ϕ80*sus*2psu3$^+$, 1.498 g/cm^3 for ϕ80dsu3$^+$, and 1.503 g/cm^3 for ϕ80*sus*2*imm*$^\lambda$psu3$^+$ in the presence of the reference phages λcI (1.508 g/cm^3) and λb2b5 (1.484 g/cm^3) (8, 9). Phage λcI was originally received from J. Weigle and λb2b5 was from G. Kellenberger. The density values 1.506 g/cm^3 for ϕ80*sus*2psu3$^+$ and 1.501 g/cm^3 for ϕ80dsu3$^+$ were reported previously (1).

Media. The media used for phage preparations were prepared as described previously (22), with the following modification. To stabilize the phage particles, the concentration of Mg^{2+} in soft agar was increased from 1 to 10 mM.

Bacteriophage preparations. For ϕ80*sus*2,

ϕ80*sus*2psu3$^+$, and ϕ80*sus*2*imm*$^\lambda$psu3$^+$, a plate stock was prepared on *E. coli* C600S, sensitive to ϕ80. For the preparation of ϕ80dsu3$^+$, the heterogenote of CA274 *lac*$^-$ amber *trp*$^-$ amber (ϕ80*sus*2) (ϕ80dsu3$^+$) was induced to yield phage by the addition of mitomycin C. The phage were pelleted, and the resuspended pellets were purified by centrifugation for 18 h in CsCl at a mean density of 1.5 g/cm^3. Centrifugation was at 23,000 rpm and 20 C in a Beckman SW39 rotor or at 21,000 rpm in a Beckman SW50.1 rotor.

Electron microscopy of DNA heteroduplexes. Preparation of denatured ϕ80 DNA by simultaneous lysis and denaturation with alkali was not satisfactory for heteroduplex formation. The presence of phage ghosts or phage protein interfered with electron microscopy. In our procedure, therefore, the purified phage stock containing CsCl was dialyzed against 0.002 M EDTA (pH 8.1), and DNA was extracted with phenol. The DNA solution was dialyzed in 0.1 × SSC (1× SSC:0.015 M NaCl and 0.0015 M sodium citrate) to remove phenol and was stored at 4 C. Single-stranded circular DNA (fdss DNA) and relaxed duplex circular DNA (fdRFII DNA) of phage fd were supplied by T. Takanami. The DNA concentration was estimated from its absorbance at 260 nm.

DNA heteroduplexes were prepared and mounted for electron microscopy by the formamide technique of Sharp et al. (18) with some modifications. The heteroduplex DNA (1.5 μg/ml) was dialyzed against 100 ml of a solution containing 0.1 M Tris (pH 8.5), 0.01 M EDTA, and 50% formamide for 2 h at 4 C. The spreading solution (per 48 μl) contained: dialyzed heteroduplex DNA, 10 μl; dialysate, 25 μl; fdss DNA (3 μg/ml), 2.5 μl; fdRFII DNA (3 μg/ml), 2.5 μl; formamide, 5 μl; and cytochrome *c* solution (1 mg/ml in 0.1 M Tris [pH 8.5] and 0.01 M EDTA), 3 μl. The final concentration of formamide was 47% in the spreading solution. The hypophase contained 0.01 M Tris (pH 8.5) and 0.001 M EDTA in 18% formamide. A 1.15-ml volume of hypophase solution was placed in a Teflon cup (diameter, 1.9 cm; depth, 0.1 cm). A clean, stainless-steel spatula was inserted, at an angle of about 45°, into the side of the hypophase drop. Spreading solution (48 μl) was then applied, through a capillary tube, onto the surface of the spatula, which was carefully removed after most of the solution had drained down.

Micrographs were taken in a JEM-7A electron microscope at an instrumental magnification of 10,000-fold, and at least 20 heteroduplexes were traced on a 10-fold-enlarged image with a Nikon 6F projection comparator. Lengths, referred to in terms of the fractional length of ϕ80 DNA, were calculated relative to the average length of several relaxed circles of fdRFII DNA and single-stranded circles of fdss DNA appearing in the same photograph with the DNA heteroduplexes. fdRFII DNA served as a duplex DNA standard, and fdss DNA served as a single-strand length standard. The ratio of the length of fdRFII DNA to the length of ϕ80*sus*2 DNA was 0.140 ± 0.005. A careful, direct comparison of fdRFII DNA with wild-type λ DNA, using the aqueous technique of Davis et al. (5), gives a value of 0.133 ± 0.003 for the length ratio, suggesting that the molecular weight of fdRFII DNA is 4.09 × 10^6 u, corresponding to 6,200 base pairs. The molecular weight of wild-type λ DNA is taken as 30.8 × 10^6 u, which corresponds to 46,500 base pairs (4).

RESULTS

Structure of ϕ80*sus*2*imm*$^\lambda$psu3$^+$ DNA. Heteroduplexes of ϕ80*sus*2*imm*$^\lambda$psu3$^+$ DNA with ϕ80*sus*2 DNA were analyzed. In this heteroduplex (Fig. 1) we observed an insertion loop and a substitution bubble corresponding to the immunity region. The substitution of the immunity region can be clearly located on the right arm of the ϕ80 DNA. Since ϕ80*sus*2imm$^\lambda$psu3$^+$ is less dense by 0.001 g/cm^3 than ϕ80*sus*2psu3$^+$, the short arm of the substitution bubble must contain the λ immunity region and the long arm must contain the ϕ80 immunity region. During vegetative growth, ϕ80*sus*2*imm*$^\lambda$psu3$^+$ produces less-dense progeny phages, ϕ80*sus*-2*imm*$^\lambda$ (1.492 g/cm^3), which have lost suppressor activity. Therefore, the insertion loop located on the left arm corresponds to the transducing bacterial region containing the su3$^+$ gene. Taking the fdss DNA as the reference, lengths of the insertion loop, the short arm of the substitution bubble, and the long arm were measured as 0.087 ± 0.011, 0.231 ± 0.034, and 0.251 ± 0.034, respectively. Duplex DNA lengths from the left terminus of the molecule to the left end of the substitution (A) and from the right end of the substitution to the right terminus of the molecule (B) were measured. The length ratio of A to B was calculated as 4.316 ± 0.215. The total length of A plus B is equal to 0.749 ϕ80 unit (= 1.000 minus the length of the long arm, 0.251). From the length ratio and the total length of A plus B, the lengths of A and B can be calculated. The left-end (x_1) and right-end (x_2) points of the substitution measured from the left terminus of the molecule were specified as 0.608 and 0.859, respectively. These points correspond to the known ϕ80/λ crossover points (6). The precise location of the insertion loop will be examined below.

Structure of ϕ80*sus*2psu3$^+$ DNA. To determine the location of the insertion loop containing the su3$^+$ gene on the left arm of ϕ80, the heteroduplexes of ϕ80*sus*2psu3$^+$ DNA with ϕ80*sus*2 DNA were examined (Fig. 2) in the presence of reference DNA molecules fdss and fdRFII. Measured duplex lengths from the left terminus of the molecule to the insertion loop (C) and to the right terminus (D) were 1.249 ± 0.142 and 15.160 ± 0.156 μm, respectively. The fdRFII DNA added as an internal duplex standard was 2.126 ± 0.068 μm long. The average length distributions of the C region and fdRFII DNA are shown by a histogram (Fig. 3a). Although there is an intrinsic fluctuation in the

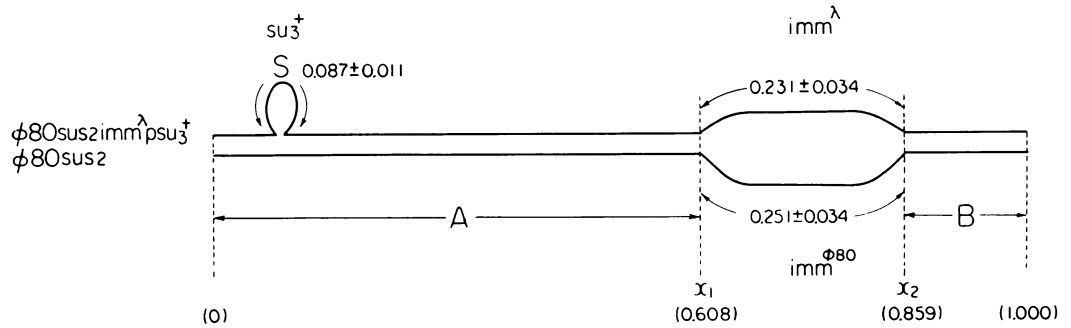

FIG. 1. *Structure of the φ80sus2imm λ psu3+/φ80sus2 heteroduplex. Capital letters represent DNA regions, whereas the lower-case letters (x) indicate substitution end points measured from the left terminus of the molecule. An insertion loop is shown by the letter S. All dimensions quoted are in φ80 units (1 φ80 unit = 44,200 base pairs = 7.14 fd unit).*

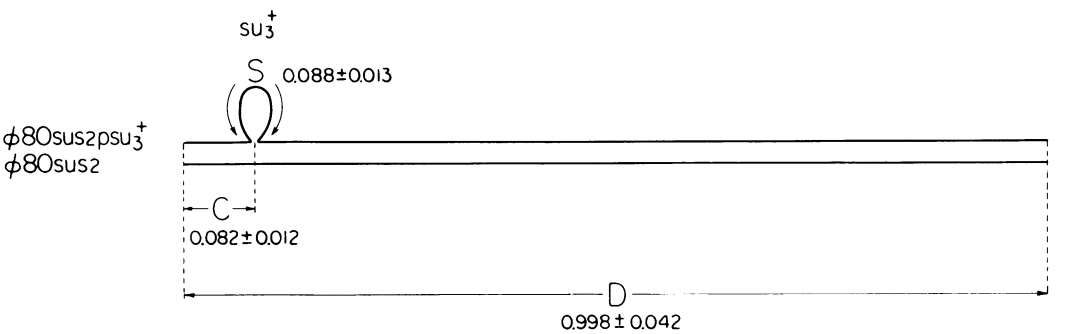

FIG. 2. *Structure of the φ80sus2psu3+/φ80sus2 heteroduplex. See the legend to Fig. 1.*

length of a duplex DNA, the standard deviation (σd) is empirically proportional to the square root of the mean length of the DNA ($\sqrt{\langle \overline{Ld} \rangle}$) (5). Standard deviations of the present length measurements for duplex DNA were plotted against the square root of the mean length in Fig. 4. The points include the C region, the D region, fdRFII DNA, and various duplex segments of φ80 heteroduplexes shown in Fig. 2 and 6. Length measurements are given in micrometers. It is seen that the ratio of σd to $\sqrt{\langle \overline{Ld} \rangle}$ is approximately 0.048 for each point except the C region (Fig. 4). The solid line shows the ratio. Only the plot for C deviates very much from the other plots, and the standard deviation measured for the C region is 2.68 times larger than that expected from the solid line, as explained in the legend to Fig. 4. Therefore, true length heterogeneity for C, such as the presence of incomplete heteroduplexes or the presence of the movable insertion loop, should be suspected. However, the total duplex length in the heteroduplex (D) shows the normal standard deviation expected from the solid line as shown in Fig. 4, and the heteroduplex shown in Fig. 2 should be complete. Therefore, it is possible that the presence of su3+-containing host DNA flanked by a homologous short segment of phage DNA gives rise to movable insertion loops. The position of the insertion loop is approximately 0.082 ± 0.012 from the left terminus of the molecule (Fig. 2). This suggests that the proposed movable distance of the insertion loop must be within ±1.2% of the φ80 length or about 2% φ80 unit.

Intrinsic length fluctuations similar to those found for double-stranded DNA are also seen for single-stranded DNA, although intrinsic variability in the length measurement increased for the single-stranded DNA. Measured single-strand lengths for the insertion loop (S) and fdss DNA are 1.080 ± 0.085 and 1.726 ± 0.113 μm, respectively. Average length distributions of insertion loop and fdss DNA are shown by the histogram (Fig. 3b). Similar plots of the standard deviation of length (σs) against the square root of the mean length ($\sqrt{\langle \overline{Ls} \rangle}$) for these single-stranded DNA and various single-stranded segments of φ80 heteroduplexes are also shown in Fig. 4. The ratio of σs to $\sqrt{\langle \overline{Ls} \rangle}$ is approximately 0.081 if single-strand lengths are given in micrometers. The dotted line shows the ratio. Since the length for the insertion loop shows the normal standard deviation

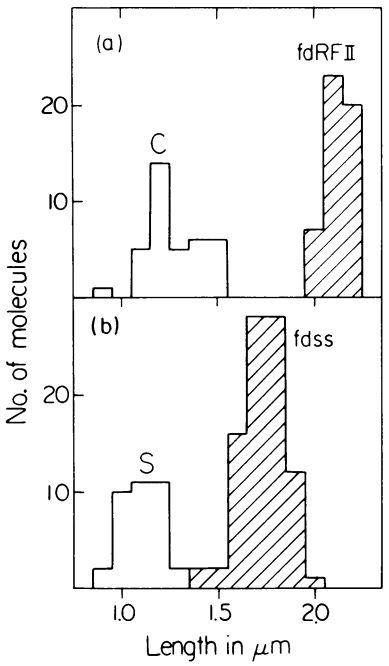

FIG. 3. *Histogram of length measurements of the segments C and S in the heteroduplex shown in Fig. 2 and the reference molecules fdRFII and fdss.*

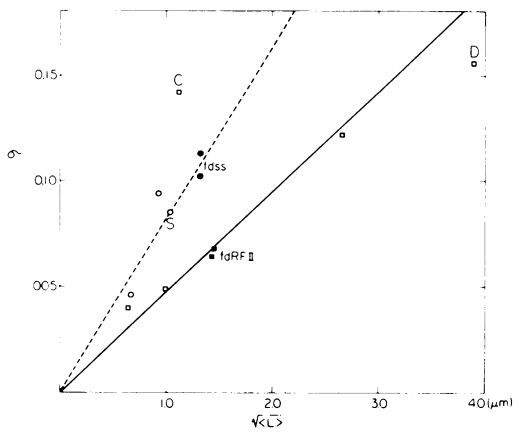

FIG. 4. *Plot of standard deviation (σ) of length measurements for samples of double-stranded DNA (□, ■) and single-stranded DNA (○, ●) versus the square root of the mean length $\langle L \rangle$. The points include fdRFII (■), fdss (●), and various segments of the heteroduplexes (□, ○) shown in Fig. 2 and 6. The letters C, D, and S denote the segments depicted in Fig. 2. Each point represents at least 20 measurements given in micrometers. The mean value of ratios of σ to $\sqrt{\langle L \rangle}$ is 0.048 for all points of duplex DNA, except for the C region and 0.081 for all points of single-stranded DNA. The solid line shows the ratio for the duplex DNA and the dotted line shows the ratio for the single-stranded DNA. The standard deviation measured for the C region is 2.68 times larger than the value expected from the solid line. This gives a difference of 7.18 times in its variance. According to Fisher's testing of statistical hypothesis, the value 7.18 is much larger than $F^{19}_{19}(0.01) = 3.03$ derived from the table of F distribution. Therefore, population variance for C is different from that expected from the solid line, with a 99% confidence probability.*

expected from the dotted line in Fig. 4, the insertion loop should have a fixed length.

Structure of ϕ80dsu3$^+$ DNA. The defective phage ϕ80dsu3$^+$ (1.498 g/cm^3) is more dense than ϕ80*sus*2 (1.493 g/cm^3) in CsCl. Therefore, ϕ80dsu3$^+$ should contain more DNA than ϕ80. The heteroduplexes of ϕ80dsu3$^+$ DNA with ϕ80*sus*2 DNA are shown in Fig. 5 and 7a. As can be seen, there is a large substitution bubble. The long arm of the substitution must represent the host chromosomal segment containing the su3$^+$ gene, and the short arm must represent the ϕ80 DNA. In ϕ80dsu3$^+$, one of the phage tail genes, gene *8*, was found to be lost by a complementation test, but ϕ80 immunity was still retained. From this result the substitution bubble could be located at the left arm of the ϕ80 DNA molecule. In the presence of fdRFII DNA as the reference, the duplex length from the left terminus to the beginning of the substitution (E) and that from the right end of the substitution to the right terminus (G) were measured as 0.028 ± 0.002 and 0.472 ± 0.013, respectively. The length of the short arm of the substitution (F1) can be computed by subtracting the value E + G from the total length. The length of F2 was computed by taking the average ratio of F2 to F1 (1.071 ± 0.0325) and multiplying it by the length of F1. These data are shown in Fig. 5.

Heteroduplexes of ϕ80*sus*2psu3$^+$ DNA with ϕ80dsu3$^+$ DNA. To specify the common region of the host chromosomal DNA contained in ϕ80dsu3$^+$ and carried by ϕ80*sus*2psu3$^+$, heteroduplexes between these two phage DNAs were formed (Fig. 6 and 7b). Two substitution bubbles of different sizes were seen in this heteroduplex. Lengths of each segment of the heteroduplex were measured with the internal reference molecules of fdRFII and fdss, and the values are given in Fig. 6. The assignment of each arm of the substitution bubbles to these two phages was made by comparing the sum of each segment length with the total lengths of these two phage DNAs shown in Fig. 2 and 5. Duplex segment I flanked by two substitution bubbles represents the bacterial chromosomal region carried by ϕ80*sus*2psu3$^+$. The length of I (0.067 ± 0.005) is 0.020 shorter than that of the insertion loop (S) shown in Fig. 1 and 2. Therefore, the insertion loop of 0.087 ϕ80 unit must

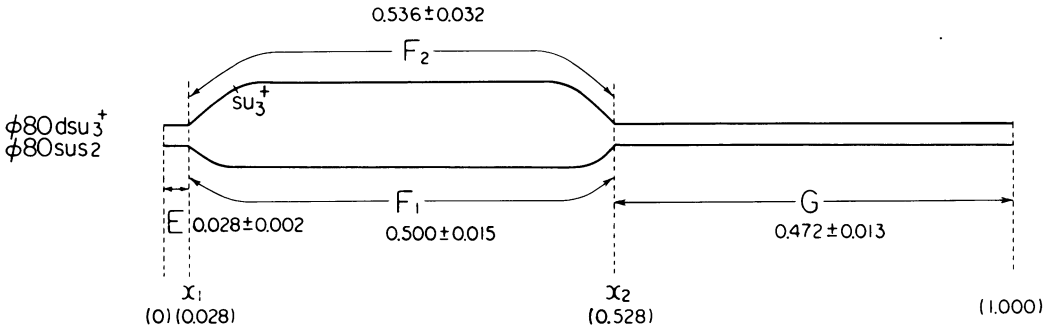

FIG. 5. *Structure of the φ80dsu3⁺/φ80sus2 heteroduplex. See the legend to Fig. 1.*

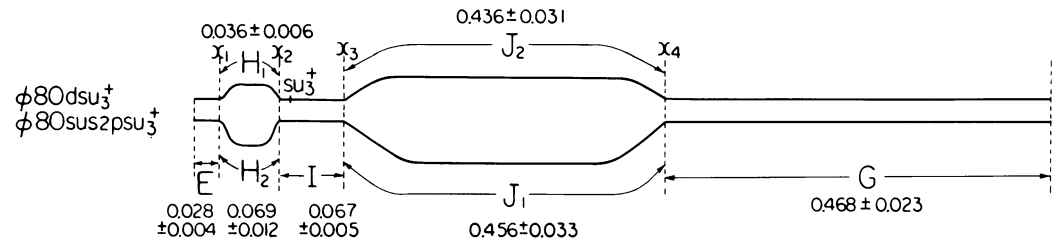

FIG. 6. *Structure of the φ80dsu3⁺/φ80sus2psu3⁺ heteroduplex. See the legend to Fig. 1.*

contain two different kinds of DNA: the bacterial DNA of 0.067 φ80 unit and the phage DNA of 0.020 φ80 unit.

DISCUSSION

The structures of φ80*sus*2, φ80dsu3⁺, φ80*sus*2psu3⁺, and φ80*sus*2*imm*λpsu3⁺ are summarized in Fig. 8. Lengths are given in fractional lengths of φ80 DNA. Direct comparison with λ using the aqueous technique of Davis et al. (5) gave a value of 0.953 ± 0.023 for the length ratio of wild-type φ80 to wild-type λ (A. Murakami and H. Yamagishi, unpublished data). In the present study, we find that the length ratio of fdRFII DNA to φ80*sus*2 DNA is 0.140 ± 0.005 and to wild-type λ DNA is 0.133 ± 0.003. Thus, the length ratio of the φ80*sus*2 DNA to wild-type λ DNA is calculated to be 0.950 ± 0.055 or 95% λ unit. The weight-average molecular weight of φ80 DNA estimated from the sedimentation rate is 95% of the λ DNA (21). However, there is some confusion with respect to φ80 DNA length. According to Fiandt et al. (6), the total length of φ80 DNA is equivalent to 92% λ unit. Ohtsubo et al. (13) report that φ80 DNA length is 43.5 kilobases, whereas the λ DNA length is 46.5 kilobases. This gives a value of 93.5% λ unit for the φ80 DNA length. The disagreement with respect to φ80 DNA length may reflect the difference of the φ80 strain used. For the length of φ80 DNA used in the present study, we take 95% λ unit, suggesting 29.26×10^6 u or 44,200 base pairs.

A distinguishing characteristic of the DNA structure of φ80*sus*2psu3⁺ is the presence of the homologous segments of phage DNA flanking the inserted bacterial segment containing the su3⁺ gene (Fig. 7). Thus, the prediction made originally by Andoh and Ozeki (1) can now be visualized, and the frequent loss of the suppressor activity during the vegetative growth of this transducing phage may be explained by the recombination between duplicated homologous regions of the phage genome. Genetic consequences of this novel structure have been studied (H. Yamagishi, H. Inokuchi and H. Ozeki, manuscript submitted for publication).

The gross gene arrangement of φ80 is similar to that of phage λ (16, 17). According to the results of complementation tests (H. Inokuchi and H. Ozeki, unpublished data), detailed arrangement of the φ80 head genes *2*, *3*, and 5 is the same as that of the λ head genes *A*, *B*, and C. Therefore, assignment of the duplicated region of the φ80 phage genome on the physical map of λ genes could be possible by locating the regions of homology between the DNAs of λ and φ80 (6). Loci of φ80 genes are tentatively shown on the φ80*sus*2 DNA molecules in Fig. 8. This figure suggests that the duplicated φ80 DNA in φ80*sus*2psu3⁺ contains a part of gene *4*. According to a study by Parkinson (14) of polar effects, it is suggested that the λ gene cluster of *W*, *B*, and C forms one operon, which is transcribed in this order. If this is the case for φ80 genes *3*, *4*, and 5, the presence of a foreign DNA inserted between duplicated fragments of a structural

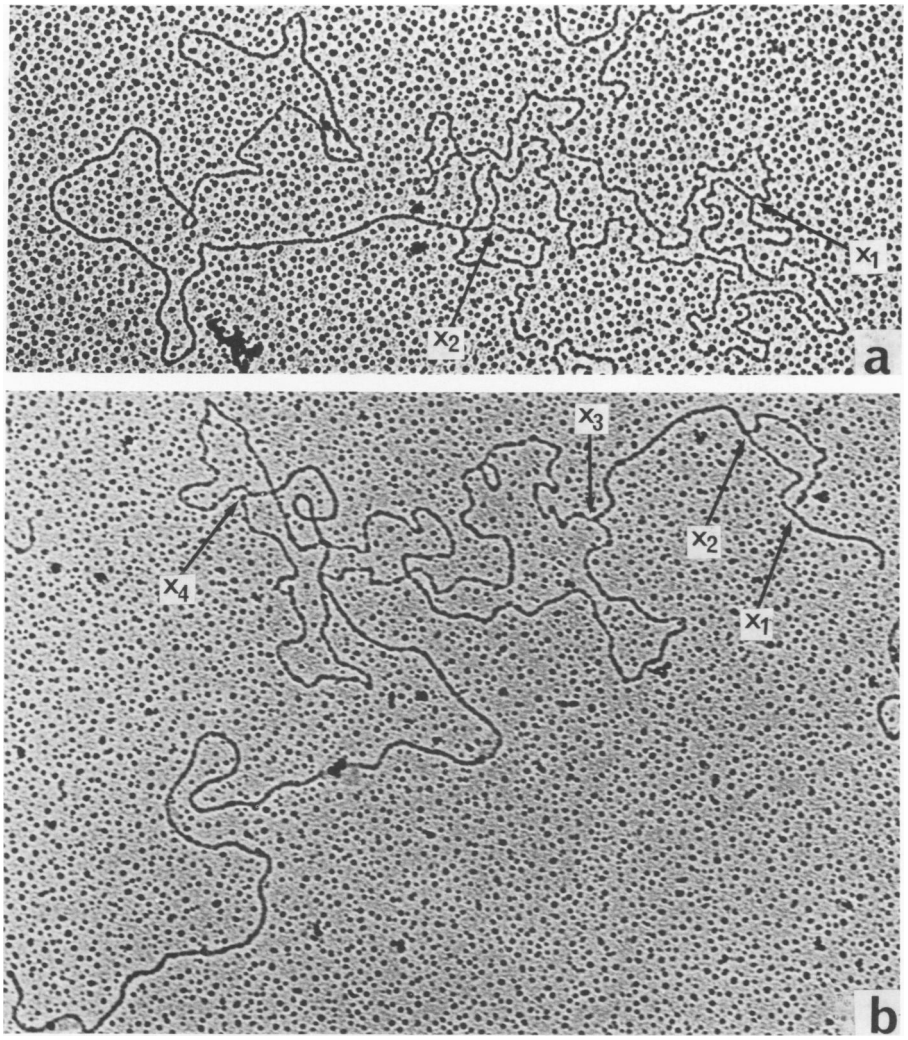

FIG. 7. *Electron micrographs of the ϕ80dsu3$^+$/ϕ80sus2 heteroduplex (a) and the ϕ80dsu3$^+$/ϕ80sus2psu3$^+$ heteroduplex (b). Total magnification is ×31,600. The schematic representation and the letter symbols are shown in Fig. 5 and 6.*

gene would reduce the expression of distal genes of the same operon. According to our preliminary study (A. Murakami, H. Inokuchi, and H. Yamagishi, Jpn. J. Genet., in press), all late genes from *4* to *13*, presumably located at the right of the transducing fragment, are partly inactivated. Polar mutations caused by the insertion of DNA have been reported for bacteriophage Mu (2, 11, 20), insertion (IS) DNA (7) and bacteriophage λ (19).

Andoh and Ozeki (1) originally isolated ϕ80*sus*2psu3$^+$ by induction of a heterogenote carrying ϕ80*sus*2 and ϕ80dsu3$^+$. However, as shown in Fig. 8, the transducing fragment carried by ϕ80*sus*2psu3$^+$ originates from the inside region of the transducing fragment of the defective phage ϕ80dsu3$^+$. This suggests that at least two illegitimate recombination events should occur in a heterogenote for the formation of ϕ80*sus*2psu3$^+$.

Miller et al. (12) and Fiandt et al. (6) specified the position of the su3$^+$ gene in the *E. coli* genome as approximately 48% λ unit or 24,000 base pairs to the left of the ϕ80 prophage attachment site. In the present study, the heteroduplex ϕ80dsu3$^+$/ϕ80*sus*2psu3$^+$ provided information on the position of the su3$^+$-containing segment derived from ϕ80*sus*2psu3$^+$ on the *E. coli* DNA carried by ϕ80dsu3$^+$. A short su3$^+$-fragment of 6.4% λ unit (6.7% ϕ80 unit) is located in the region between 47.7 and 41.3% λ unit (50.2 and 43.5% ϕ80 unit) to the left of the

ϕ80 prophage attachment site (Fig. 8). The value of 47.7% λ unit is very close to 48% λ unit, the distance from the ϕ80 attachment site to the su3$^+$ gene. This suggests that the sus3$^+$ gene is located at the very left distal end on the *E. coli* fragment carried by ϕ80*sus*2psu3$^+$.

The orientation of tRNA transcription for the two strains of plaque-forming transducing phages carrying the su3$^+$ gene is summarized in Fig. 9 (3, 10, 12). It is noteworthy that in both phages the orientation of the su3$^+$ gene transcription is always different from that of mRNA transcription on the neighboring phage genome. This suggests that the su3$^+$ gene transcription should initiate on its own promoter and that su3$^+$ transcription by the read-through mechanism may be unlikely. In fact, gene expression of su3$^+$ is observed in the lyso-

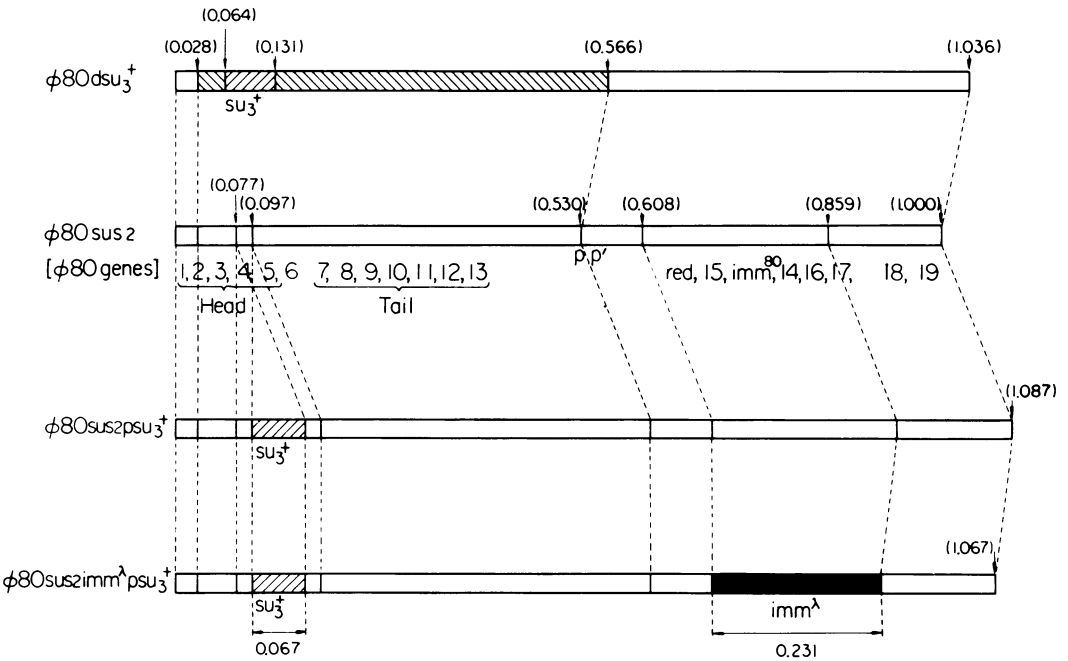

FIG. 8. *Summary of experimental data for the determination of the structure of ϕ80sus2, ϕ80dsu3$^+$, ϕ80sus2psu3$^+$, and ϕ80sus2imm$^\lambda$psu3$^+$. Open rectangles, ϕ80 phage DNA; solid rectangle, λ phage DNA; hatched rectangles, bacterial DNA. Dotted lines represent the correspondence of the regions.*

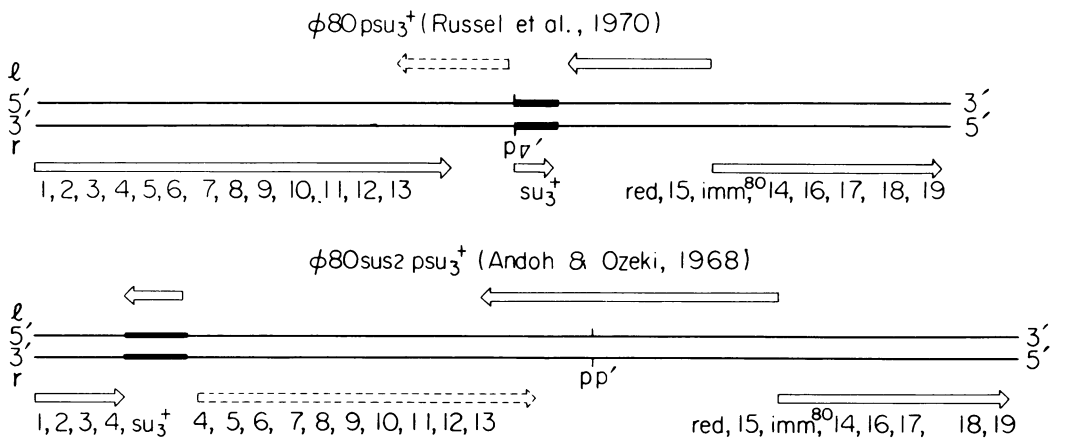

FIG. 9. *Orientation of transcription for phages ϕ80psu3$^+$ (15) and ϕ80sus2psu3$^+$ (1). The orientation of transcription is indicated by arrows (3, 10, 12).*

genic state and the induced state.

ACKNOWLEDGMENTS

We wish to thank John Milton for reading the manuscript.

This work was supported by a Grant-in-Aid for Scientific Research and for Cancer Research from the Ministry of Education, Science and Culture, Japan.

LITERATURE CITED

1. **Andoh, T., and H. Ozeki.** 1968. Suppressor gene su3+ of *E. coli*, a structural gene for tyrosine tRNA. Proc. Natl. Acad. Sci. U.S.A. 59:792-799.
2. **Boram, W., and J. Abelson.** 1971. Bacteriophage Mu integration: on the mechanism of Mu-induced mutations. J. Mol. Biol. 62:171-178.
3. **Daniel, V., J. S. Beckman, S. Sarid, J. I. Grimberg, M. Hertzberg, and U. Z. Littauer.** 1971. Purification and in vitro transcription of a transfer RNA gene. Proc. Natl. Acad. U.S.A. 68:2268-2272.
4. **Davidson, N., and W. Szybalski.** 1971. Physical and chemical characteristics of lambda DNA, p. 45-82. *In* A. D. Hershey (ed.), The bacteriophage lambda. Cold Spring Harbor Laboratory, Cold Spring Harbor, N.Y.
5. **Davis, R. W., M. Simon, and N. Davidson.** 1971. Electron microscope heteroduplex methods for mapping of base sequence homology in nucleic acids, p. 413-428. *In* L. Grossman and K. Moldave (ed.), Methods in enzymology, vol. 21. Academic Press Inc., New York.
6. **Fiandt, M., Z. Hradecna, H. A. Lozeron, and W. Szybalski.** 1971. Electron micrographic mapping of deletions, insertions, inversions, and homologies in the DNAs of coliphages lambda and phi 80, p. 329-354. *In* A. D. Hershey (ed.), The bacteriophage lambda. Cold Spring Harbor Laboratory, Cold Spring Harbor, N.Y.
7. **Hirsch, H. J., H. Saedler, and P. Starlinger.** 1972. Insertion mutations in the control region of the galactose operon of *E. coli*. II. Physical characterization of the mutation. Mol. Gen. Genet. 115:266-276.
8. **Kellenberger, G., M. L. Zichichi, and J. Weigle.** 1960. Mutations affecting the density of bacteriophage λ. Nature (London) 187:161-162.
9. **Kellenberger, G., M. L. Zichichi, and J. Weigle.** 1961. Exchange of DNA in the recombination of bacteriophage λ. Proc. Natl. Acad. Sci. U.S.A. 47:869-878.
10. **Lozeron, H. A., and W. Szybalski.** 1969. Congruent transcriptional controls and heterology of base sequences in coliphage λ and φ80. Virology 39:373-378.
11. **Martuscelli, J., A. L. Taylor, D. J. Cummings, V. A. Chapman, S. S. DeLong, and L. Cañedo.** 1971. Electron microscopic evidence for linear insertion of bacteriophage Mu-1 in lysogenic bacteria. J. Virol. 8:551-563.
12. **Miller, R. C., P. Besmer, H. G. Khorana, M. Fiandt, and W. Szybalski.** 1971. Studies on polynucleotides. XLVII. Opposing orientations and location of the su+III gene in the transducing coliphages φ80psu+III and φ80dsu+IIIsu-III. J. Mol. Biol. 56:363-368.
13. **Ohtsubo, E., H. J. Lee, R. C. Deonier, and N. Davidson.** 1974. Electron microscope heteroduplex studies of sequence relations among plasmids of *Escherichia coli*. VI. Mapping of F14 sequences homologous to φ80d*met*BJF and φ80d*arg*ECBH bacteriophages. J. Mol. Biol. 89:599-618.
14. **Parkinson, J. S.** 1968. Genetics of the left arm of the chromosome of bacteriophage lambda. Genetics 59:311-325.
15. **Russell, R. L., J. N. Abelson, A. Landy, M. L. Gefter, S. Brenner, and J. D. Smith.** 1970. Duplicate genes for tyrosine transfer RNA in *Escherichia coli*. J. Mol. Biol. 47:1-13.
16. **Sato, K.** 1970. Genetic map of bacteriophage φ80: gene J on the right arm. Virology 40:1067-1069.
17. **Sato, K., Y. Nishimune, M. Sato, R. Numich, A. Matsushiro, H. Inokuchi, and H. Ozeki.** 1968. Suppressor-sensitive mutants of coliphage φ80. Virology 34:637-649.
18. **Sharp, P. A., M. T. Hsu, E. Ohtsubo, and N. Davidson.** 1972. Electron microscope heteroduplex studies of sequence relations among plasmids of *Escherichia coli*. I. Structure of F-prime factors. J. Mol. Biol. 71:471-497.
19. **Shimada, K., R. A. Weisberg, and M. E. Gottesman.** 1973. Prophage lambda at unusual chromosomal locations. II. Mutations induced by bacteriophage lambda in *Escherichia coli* K12. J. Mol. Biol. 80:297-314.
20. **Taylor, A. L.** 1963. Bacteriophage-induced mutation in *Escherichia coli*. Proc. Natl. Acad. Sci. U.S.A. 50:1043-1051.
21. **Yamagishi, H., K. Nakamura, and H. Ozeki.** 1965. Cohesion occurring between DNA molecules of temperate phages φ80 and lambda or φ81. Biochem. Biophys. Res. Commun. 20:727-732.
22. **Yamagishi, H., and H. Ozeki.** 1972. Comparative study of thermal inactivation of phage φ80 and lambda. Virology 48:316-322.